DENTAL MATERIALS 35 (2019) 1073–1081

Available online at www.sciencedirect.com

ScienceDirect

journal homepage: www.intl.elsevierhealth.com/journals/dema

Physicochemical and morphological characterization of a glass ceramic treated with different ceramic primers and post-silanization protocols

Marina Barrêto Pereira Moreno[a], *Fabián Murillo-Gómez*[b], *Mario Fernando de Goes*[a,*]

[a] *Dental Materials Division, Department of Restorative Dentistry, Piracicaba Dental School, State University of Campinas – UNICAMP, Av Limeira 901, Areiao, Piracicaba, SP, 13414–903, Brazil*

[b] *Department of Restorative Dentistry, School of Dentistry, University of Costa Rica, San José, Costa Rica*

ARTICLE INFO

Article history:
Received 20 February 2019
Accepted 3 May 2019

Keywords:
Silane
Self-Etching ceramic primer
Glass ceramic
Scanning electron microscopy
Chemical analysis

ABSTRACT

Objective. Evaluate the effect of different ceramic primers and post-silanization protocols on physicochemical and morphological characteristics of a lithium disilicate glass ceramic.

Methods. Lithium disilicate ceramic (IPS e-max CAD) plaques (6 × 10 × 2 mm) were divided into 3 groups according to the ceramic primer used: (1) Silane (RelyX Ceramic Primer-RL); (2) Silane + MDP (Clearfil Ceramic Primer Plus-CP); (3) Self-etching ceramic primer (Monobond Etch and Prime-MB). Specimens from each group were distributed into 5 sub-groups according to post-silanization protocols: (a) Treated as recommended by the manufacturer (MR), (b) MR + Additional drying with air at room temperature for 30 s (RTA), (c) MR + additional drying with hot air for 30 s (HT), (d) MR + Surface rinsing with water at room temperature for 10 s and drying with air at room temperature for 30 s (WT), and (e) Specimens were not silanized (NS). Surface free energy (SFE) was determined using static contact angles measurements with water and diiodomethane. SFE data were submitted to Friedman followed by Wilcoxon post-hoc test ($\alpha = 0.05$). Morphology was analyzed using scanning electron microscopy. Elemental composition and chemical interactions were determined with X-ray photoelectron spectroscopy analysis.

Results. RL presented the highest SFE (62.4 mN/m) followed by CP (59.7 mN/m). Post-silanization protocols resulted in similar SFE, but WT and HT induced the highest water contact angles when using CP and RL. CP modified ceramics' surface morphology compared to the etched and RL treated groups. The presence of water was identified on CP treated specimen. All analyzed primers formed siloxane bonds with ceramic surface.

Significance. Ceramic primers resulted in different surface free energy and morphology, but siloxane bonds were identified for all tested solutions. HT and WT protocols should be used with RL and CP primers. MB was not influenced by the different silanization protocols.

* *Corresponding author at*: Piracicaba Dental School – University of Campinas (FOP-UNICAMP), Dental Materials Division, Av Limeira 901, Areiao, Piracicaba, SP, 13414–903, Brazil.

E-mail addresses: marinabpmoreno@hotmail.com (M.B.P. Moreno), fabian.murillogomez@ucr.ac.cr (F. Murillo-Gómez), degoes@unicamp.br (M.F. de Goes).

https://doi.org/10.1016/j.dental.2019.05.003

1. Introduction

A wide range of ceramics with different compositions and processing techniques are now available for indirect restorations [1,2]. Different classification systems have been proposed. For example, dental ceramics can be classified according to the glass content on its chemical composition as polycrystalline or glass ceramics [3]. Lithium disilicate glass ceramics are mainly composed of a silica rich phase reinforced with crystals and have been widely used due to optimal mechanical properties and aesthetics [2,4]. Moreover, they can be adhesively luted to the tooth structure. A strong and long-lasting bond with resin cement depends on the performance of a proper ceramic surface treatment [2,3,5]. Two main approaches have been recommended to prepare the ceramic restoration: micromechanical retention and chemical bond [3]. Hydrofluoric acid changes surface topography as it selectively attacks the glassy phase increasing surface energy and creating microporosities which facilitate micromechanical interlocking of the resin cement [2,3]. On the other hand, silane coupling agents act as mediators and promote chemical bonding of the resin cement with the ceramic surface [1].

Silanes consist on organic compounds that essentially contain one or more silicon atoms [6]. The most common type used in dentistry is ɣ-methacryloxypropyltrimethoxysilane (MPTS). It is a bifunctional molecule with one organofunctional group containing methyl methacrylate that copolymerize with resin cements and hydrolysable alcoxy groups that reacts with Si–OH on the ceramic surface [1,7]. The alcoxy groups must first be activated via hydrolysis (SiOR→SiOH) in order to be suitable to chemically react with ceramic material [8,9]. The silanol group suffers a condensation reaction with hydroxyls present on the ceramic, releasing water as a byproduct [10]. MPTS also reacts within to form siloxane bonds by horizontal condensation, resulting in a cross-linking tridimensional layer [11]. The formation of this branched hydrophobic layer increases hydrolytic stability and makes the ceramic surface more prone to bond resin materials [5,12].

The structure of the silane layer is influenced by a number of factors such as composition of the silane solution and post-silanization protocols [13]. These protocols should remove water, solvents and contaminants in order to increase the accessible sites on ceramic surface to bond to MPTS molecules and enhance the condensation reactions within the silane compounds [8]. The efficiency of different protocols might vary according to each silane composition [14]. Manufacturers usually recommend the application of a mild oil-free air, but it seems that is not enough to effectively remove solvents [13,15]. The usage of heat treatment has been the main alternative treatment previously evaluated, but the effectiveness of this protocol is not yet a consensus [13,16–18].

In general, the composition of conventional silanes consists on MPTS molecules, acetic acid, ethanol and water. They are available in one bottle, which is presented in a pre-hydrolyzed solution or in a two-bottle system that should be mixed before use [10]. However, in order to obtain universal and simplified silane primers, new formulations are emerging. Multi-purpose ceramic/metal primers containing MPTS with 10-methacryloyloxydecyl dihydrogen phosphate (10-MDP) have been recently released [19–21]. The incorporation of the 10-MDP in these primers is justified by the reduced ability of silanes to form chemical bonds to zirconia and metal reason why phosphate monomers are employed along, as they have been reported to bond successfully to such substrates [22]. Therefore, they could be used with both glass ceramics and zirconia. However, some studies have demonstrated that the association of 10-MDP with silane in a single bottle resulted on deactivation of the silanol component present on MPTS molecules and consequently reducing its bonding potential [20,21]. Moreover, the effect of these primers on glass-ceramics' properties have not been clarified yet.

A new self-etching ceramic primer was also introduced claiming to etch and silanize in one step [23]. According to the manufacturer, it is composed of tetrabutylammonium dihydrogen fluoride that produces a less aggressive etching pattern compared to HF and along with a silane system based on trimethoxypropyl methacrylate they both form a strong bond with the ceramic surface [23,24]. The effectiveness of this product on ceramic-resin cement bonding is still contradictory [24–28] and detailed characterizations are scarce. Besides the inherent advantage as a simplified treatment, some aspects regarding its effect on ceramic surface and its capability to form durable siloxane bonds, require more investigations.

Thus, the aim of the present study was to evaluate the effect of different ceramic primers and post-silanization protocols on surface energy and morphology of a lithium disilicate glass ceramic and on the chemical composition and interaction of the silane layer formed on ceramics' surface. The null hypotheses tested in this study are that: (1) there are no significant differences on surface free energy of ceramics treated with different ceramic primers and post-silanization protocols; (2) there are no significant differences on surface morphology of ceramics treated with different ceramic primers and post-silanization protocols; (3) the resultant composition and chemical interaction of the silane layer is not different among ceramic primers and post-silanization protocols.

2. Materials and methods

2.1. *Surface free energy (SFE) and contact angle measurements*

Ceramic plaques (6 × 10 × 2 mm) were cut from pre-sintered lithium disilicate CAD/CAM blocks (IPS e-max CAD, Ivoclar Vivadent, Schaan, Liechtenstein) using a diamond disk mounted in a precision cutting machine (Isomet 1000, Buehler, Lake Bluff, IL) under water irrigation. The plaques were fired according to the manufacturer's recommendations and polished under irrigation with 600-grit silicone-carbide abrasive papers (Norton AS, São Paulo, SP, Brazil) in automatic polisher (APL4, Arotec, Cotia, SP, Brazil) to standardize all surfaces. The specimens were ultrasonically cleaned in distilled water for 5 min.

Specimens were divided into 3 groups according to the ceramic primer used: (1) Silane - Rely X Ceramic Primer - RL (3M ESPE, St. Paul, MN, USA); (2) Silane + MDP - Clearfil

Table 1 – List of all materials used and their composition.

Material	Manufacturer	Lot.	Composition	Manufacturer's recommendation
Lithium disilicate reinforced glass ceramic	IPS emax CAD (Ivoclar Vivadent – Schaan, Lichtenstein)	V13056	SiO_2 (57–80%wt), Li_2O (11–19%wt), K_2O (0–13%wt), P_2O_5 (0–11%wt), ZrO_2 (0–8%wt), ZnO (0–8%wt), Al_2O_3 (0–5%wt) MgO (0–5%wt), colouring oxides (0–8%wt)	
Hydrofluoric Acid	Condac Porcelana 5% (FGM – Joinville, Brazil)	080217	Hydrofluoric acid 5%, water, thickener, surfactant, colorant	
Silane	RelyX Ceramic Primer (3M ESPE – St. Paul, USA)	N662908	Ethyl alcohol (70–80%wt), water (20–30%wt), methacryloxypropyltrimethoxysilane (<2%wt)	Apply on the ceramic surface and gently blow oil free air (the drying time was standardized as 5 s in the present study).
Single-component primer	Clearfil Ceramic Primer Plus (Kuraray Noritake Dental Inc – Okayama, Japan)	8W0029	Ethanol (>80%), 3-trimethoxysilylpropyl methacrylate (<5%), 10-Methacryloyloxydecyl dihydrogen phosphate	Apply on the ceramic surface and blow mild oil-free air (the drying time was standardized as 5 s in the present study).
Self-etching ceramic primer	Monobond Etch and Prime (Ivoclar Vivadent – Schaan, Liechtenstein)	V09353	Butanol, tetrabutylammonium dihydrogen trifluoride, methacrylated phosphoric acid ester, bis(triethoxysilyl)ethane, silane methacrylate, colourant, ethanol, water	Actively apply on the ceramic surface for 20 s, allow to react for 40 s, wash it with water and dry with a water- oil- free air for 10 s.

Ceramic Primer Plus - CP (Kuraray Noritake Dental Inc, Sakazu, Kurashiki, Okayama, Japan); (3) Self-etching ceramic primer - Monobond Etch and Prime - MB (Ivoclar Vivadent, Schaan, Liechtenstein). Materials composition and manufacturer's recommendation are described on Table 1.

The polished surface of the specimens from groups 1 and 2 were etched with 5% hydrofluoric acid (Condac Porcelana, FGM, Joinville, SC, Brazil) for 20 s. Afterwards, they were rinsed with compressed air/water spray for 60 s, ultrasonically cleaned in distilled water for 5 min and dried for 60 s.

Specimens from each group were then distributed into 5 sub-groups according to additional protocols after ceramic primer application (n = 10): (a) Only treated as recommended by manufacturer (no additional step: positive control group - MR), (b) MR + additional drying with air at room temperature for 30 s (RTA), (c) MR + additional drying with hot air for 30 s (HT) applied with a hairdryer (TAIFF, 1300 W) at 85 °C and a standard distance of 10 cm, (d) MR + surface rinsing with water at room temperature for 10 s and drying with air at room temperature for 30 s (WT), and (e) Specimens were not silanized at all (negative control group-NS). Experimental groups are described on Table 2.

Surface free energy (SFE) was calculated based on the contact angle formed on the treated ceramic surface by two liquids (water and diiodomethane) having different surface tension. A 5 μl drop of the liquid was calibrated with the aid of a syringe and placed on the ceramic surface. After 5 s, the static contact angle formed between liquid and substrate was measured using a goniometer coupled to a software (Digidrop Contact Angle Meter; GBX, Bourg de Peage, France). Two measurements in different regions of each surface were performed and an average per specimen was obtained. Surface free energy was calculated using the harmonic average formula (Eqs. (1 and 2)) [29,30]. Contact angle values and the known information related to the liquids [31] were replaced into the formulas to isolate the dispersive and polar components of the solid. The sum of these components represent the SFE (γ^{TOT}) of the solid (Eq. (3)).

$$(1+\cos\theta)\,\gamma L1^{TOT} = \frac{4\gamma S^{D}\,\gamma L1^{D}}{\gamma S^{D}+\gamma L1^{D}} + \frac{4\gamma S^{P}\gamma L1^{P}}{\gamma S^{P}+\gamma L1^{P}} \quad (1)$$

$$(1+\cos\theta)\,\gamma L2^{TOT} = \frac{4\gamma S^{D}\,\gamma L2^{D}}{\gamma S^{D}+\gamma L2^{D}} + \frac{4\gamma S^{P}\gamma L2^{P}}{\gamma S^{P}+\gamma L2^{P}} \quad (2)$$

$$SFE = \gamma S^{TOT} = \gamma S^{D} + \gamma S^{P} \quad (3)$$

Where: $\cos\theta$ = cosine of the liquid contact angle: (L1) diiodomethane and (L2) water. γL^{TOT} is the surface tension of the liquid. γL^{D} and γL^{P} are the known dispersive and polar components of the liquid, respectively. γS^{D} and γS^{P} are the components of the solid.

SFE data were not normally distributed. Non-parametric statistical analysis was performed (Minitab v17.2.1, Minitab Inc.; State College, PA, USA) using Friedman test followed by Wilcoxon post-hoc test. The level of significance was set at $\alpha = 0.05$. The contact angle values formed on the treated ceramic surface with water were also statistically analyzed. To fulfill parametric analysis requirements, data were transformed using the Box-Cox procedure through the estimation of the optimum λ value (0.390121). Normality and homoscedasticity were checked out using Anderson-Darling and Barlett tests. Then data were analyzed using two-way ANOVA followed by Tukey post-hoc test ($\alpha = 0.05$).

Table 2 – Experimental groups.

Primer	Silanization protocol
1) RL – Silane (RelyX Ceramic Primer)	a) MR – manufacturer's recommendation b) RTA – MR + additional drying with air at room temperature for 30 s c) HT – MR + additional drying with hot air for 30 s d) WT – MR + surface rinsing with water at room temperature for 10 s and drying with air at room temperature for 30 s e) NS – not silanized
2) CP – Silane + MDP (Clearfil Ceramic Primer)	a) MR – manufacturer's recommendation b) RTA – MR + additional drying with air at room temperature for 30 s c) HT – MR + additional drying with hot air for 30 s d) WT – MR + surface rinsing with water at room temperature for 10 s and drying with air at room temperature for 30 s e) NS – not silanized
3) MB – Self-etching ceramic primer (Monobond Etch and Prime)	a) MR – manufacturer's recommendation b) RTA – MR + additional drying with air at room temperature for 30 s c) HT – MR + additional drying with hot air for 30 s d) WT – MR + surface rinsing with water at room temperature for 10 s and drying with air at room temperature for 30 s e) NS – not silanized

2.2. *Surface morphology*

Lithium disilicate ceramic plaques (6 × 10 × 2 mm) were obtained as described previously and treated with the different ceramic primers and post-silanization protocols. The specimens were mounted on aluminum stubs, sputter coated with gold-palladium alloy (SCD 050; Balzers, Schaan, Liechtenstein) and analyzed under a scanning electron microscope (SEM) (JSM 5600 LV; JEOL, Tokyo, Japan) operating at 15 kV. Surface morphology of the specimens was evaluated at 5000× magnification.

2.3. *X-ray photoelectron spectroscopy (XPS) analysis*

XPS analysis was used to verify elemental composition of the silane layer and chemical bonds formed with the ceramic surface. The analysis was carried out on the Thermo K-Alpha XPS (Thermo Scientific, Inc) with a monochromatic source Al Kα, 1486 eV. The energy interval used was from 0 to 1300 eV. A pass energy of 200 eV was used to the survey scans (long scan) and to the high resolution scans (short scan) a pass energy of 50 eV was selected. The resolutions were 1 eV for long scan and 0.01 eV for short scan. The different post-silanization protocols were evaluated on ceramic surfaces treated with RL only. Groups treated with CP and MB were only analyzed when employing MR post-silanization treatment. Analysis were performed in two different points per sample for all groups and data were processed using the Thermo Scientific™ Avantage Software (Massachusetts, USA).

3. Results

3.1. *Surface free energy and contact angle measurements*

Friedman test revealed that the factors "ceramic primer" and "post-silanization protocol" were statistically significant ($p < 0.001$) for SFE data analysis. All medians and group comparisons are listed on Table 3. Specimens treated with RL presented the highest surface free energy among the analyzed ceramic primers, followed by CP groups. Regarding silanization protocols, not silanized specimes (NS) showed the highest SFE values. MR resulted in the highest SFE among the groups that received silane application but was not different from HT and WT. RTA presented the lowest SFE but was not different from HT and WT.

Table 3 – Surface Free Energy (γt in mN/m) median for all experimental groups.

	RL	CP	MB	
NS	65.2 (65.0–65.4)	65.4 (64.8–65.5)	53.7 (51.4–55.0)	62.2 A
MR	63.0 (61.8–63.7)	59.0 (56.9–60.3)	48.3 (50.5–45.3)	59.0 B
RTA	62.3 (59.4–63.2)	56.8 (55.7–58.1)	48.3 (49.5–45.8)	56.8 C
HT	61.8 (60.7–62.3)	58.7 (57.2–60.2)	47.6 (46.8–50.1)	58.7 BC
WT	61.7 (60.9–62.8)	60.8 (60.2–62.2)	47.0 (45.2–49.4)	60.8 BC
	62.4 a	59.7 b	48.3 c	

Individual factors (ceramic primer, silanization protocols) resulted on statistically significant differences. General medians from each level are displayed bellow the names (for ceramic primers) and on the right side of the rows (for silanization protocols). Minimum and maximum values are displayed in parenthesis. Different letters represent statistical differences (capital in column, lower case in row). (Wilcoxon $p < 0.05$).
Protocol abbreviations: NS — Not silanized; MR — Treated as recommended by manufacturer; RTA — MR + additional drying with air at room temperature for 30 s; HT — MR + additional drying with hot air for 30 s; WT — MR + additional surface rising with water for 10 s and drying with air at room temperature for 30 s.

Contact angles formed between water and the treated ceramic surfaces are illustrated on Fig. 1. Normality (Anderson-Darling, $p = 0.220$) and homoscedasticity (Bartlett, $p = 0.124$) were proved. ANOVA revealed that the interaction between the factors "ceramic primer" and "post-silanization protocol" was statistically significant ($p < 0.0001$). NS groups presented lower contact angles compared to silanized surfaces. Ceramic surfaces treated with MB formed higher contact angles compared to CP and RL. The protocols HT and WT increased contact angles on specimens treated with RL and CP. Manufacturer's recommendation (MR) resulted in lower contact angles for RL and was not different from not silanized specimens. Different silanization protocols presented similar contact angles within MB groups.

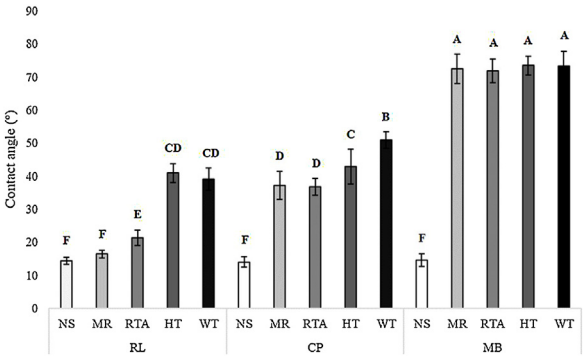

Fig. 1 – Contact angle measurements with water (°) from all experimental groups. Different letters represent statistical differences (Tukey $p < 0.05$).

3.2. *Surface morphology*

SEM images of the surface morphology produced by the different treatments are showed on Fig. 2. The non-treated (only polished) ceramic presented a homogenous and regular surface without pores and defects, but some grooves produced by the silicon-carbide abrasive paper are also evident. HF promoted the formation of an irregular surface with homogeneous distributions of microporosites and exposition of the elongated crystals. MB applied on polished surface produced a less pronounced etching pattern compared to HF with slight alteration of the ceramic surface. No difference on surface morphology was noticed after RL application on the previously etched ceramic. Conversely, CP application seems to have formed a layer and reduced the microporosites produced by HF during the previous step.

Table 4 – Elemental composition and atomic concentration (%) obtained from XPS analysis of the treated ceramic surface.

	Si 2p	O 1s	C 1s	P 2p	F 1s
RL – NS	24.13	51.04	24.83	–	–
RL – MR	19.35	40.41	40.24	–	–
RL – RTA	16.76	38.72	44.52	–	–
RL – HT	16.46	36.73	46.81	–	–
RL – WT	23.66	48.94	23.66	–	–
CP	9.01	25.17	64.73	1.08	–
MB	8.99	22.75	63.42	0.97	3.87

3.3. *X-ray photoelectron spectroscopy (XPS) analysis*

The chemical elements and atomic concentrations present on the treated ceramic surfaces were obtained through XPS survey spectra (Table 4). Si 2p was present in all groups, but in higher concentrations on the ceramic treated with RL compared to CP and MB. P 2p was identified on CP and MB groups and F 1s was present on specimens treated with MB. C 1s concentration increased after ceramic primers application compared to the not silanized specimen, except for the group RL-WT.

Fig. 3 shows the representative Si 2p high resolution spectra. The control group (not silanized) presented a single spectrum with a peak close to 103.0 eV. RL ceramic primer applied with the different silanization protocols exhibited similar spectra with peaks close to 102.5 and 103.2 eV, except for RL-MR which showed a single spectrum similar to NS. Spectra from groups CP and MB when treated following manufacturer's recommendations, presented peaks ranged from 102.2 to 103.7 eV. O 1s high resolution spectra are exhibited on Fig. 4. All analyzed groups presented a single spectrum, similar to that represented by RL-RTA, with a peak at 532.35 ± 0.2 eV. The only exception was found on groups treated with CP which showed an additional peak at 533.3 eV.

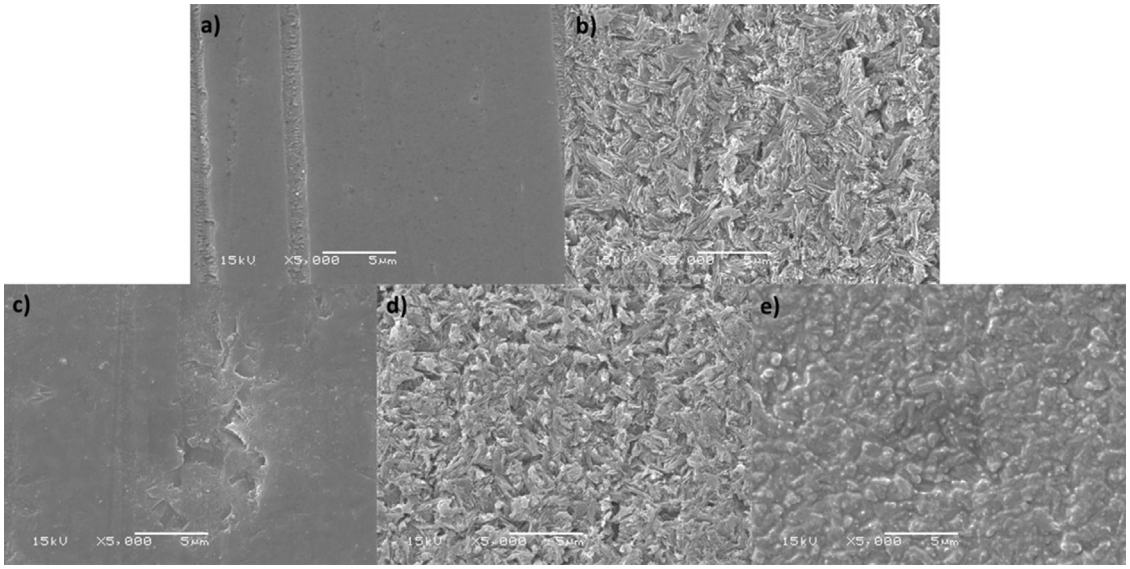

Fig. 2 – Representative SEM images from the surface morphology produced by the different treatments at 5000× magnification: (a) polished with #600 grit silicon-carbide abrasive paper (PL); (b) conditioned with hydrofluoric acid 5% for 20 s (HF); (c) PL + MB; (d) HF + RL; (e) HF + CP.

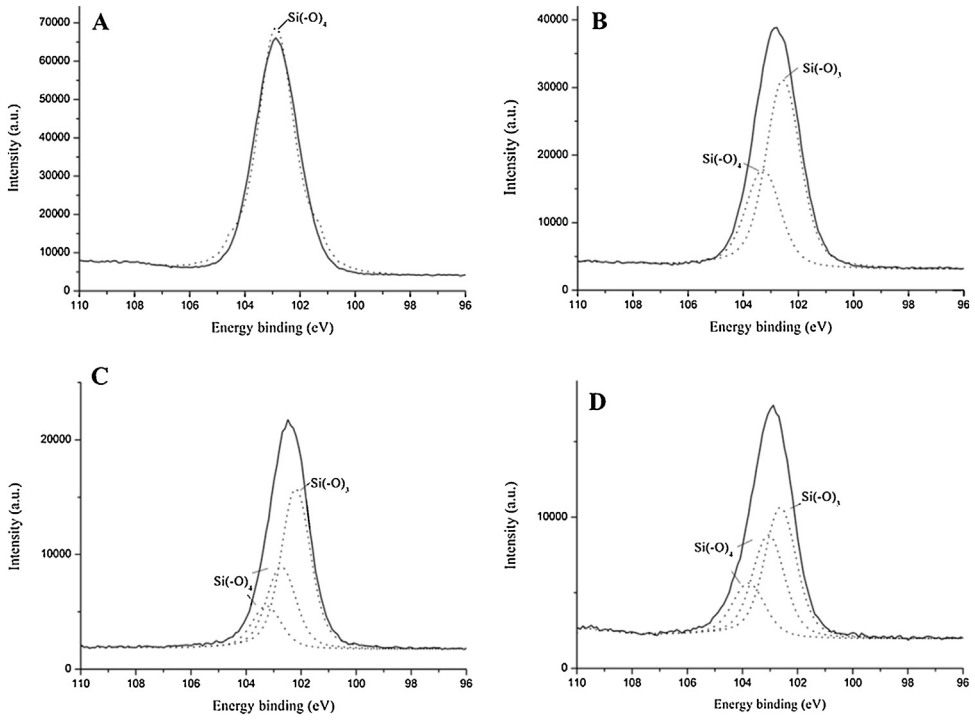

Fig. 3 – High-resolution XPS Si 2p spectra from treated ceramic surfaces (A) not silanized (NS); (B) RL applied following RTA protocol (manufacturer's recommendation + additional drying with air at room temperature for 30 s) (RL-RTA); (C) CP applied following manufacturer's recommendation (CL-MR); (D) MB applied following manufacturer's recommendation (MB-MR).

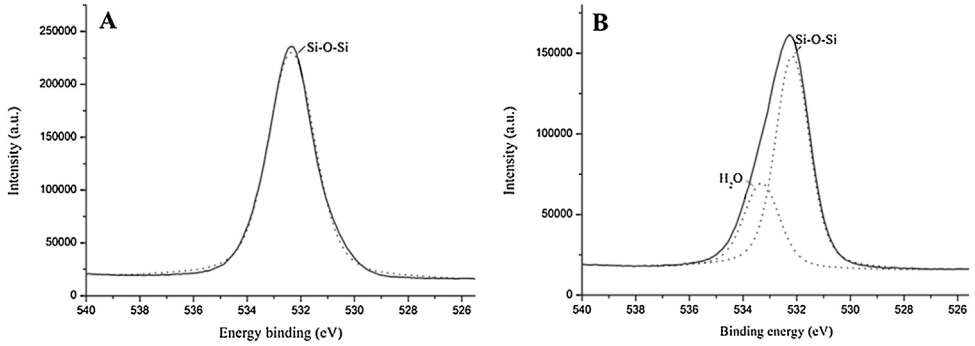

Fig. 4 – High-resolution XPS O1s spectra from treated ceramic surfaces (A) RL applied following RTA protocol (manufacturer's recommendation + additional drying with air at room temperature for 30 s) (RL-RTA); (B) CP applied following manufacturer's recommendation (CP-MR).

4. Discussion

This in vitro study evaluated the effect of ceramic primers (with different composition) and post-silanization protocols on surface characteristics of a lithium disilicate glass ceramic. Our results demonstrated that the primers and application methods significantly influenced surface free energy values, reason why the first null hypothesis must be rejected. Although silanization protocols did not result in alterations on surface morphology, the ceramic primers modified surface morphology and thus the second hypothesis must be rejected. Finally, the third hypothesis must also be rejected as the analyzed factors induced different chemical compositions and interactions with the ceramic surface.

Adhesive bonding is influenced by the surface energy of the substrate and the wettability of the adhesive [7]. At the surface, the energy is higher because the outmost atoms are not equally attracted in all directions [7]. A high surface energy is desired as it favors the spreading of the silane primer, adhesive system or resin cement across the ceramic surface [32]. A higher wettability of a liquid maximizes its contact capability and attractive forces towards the substrate, which is an important requirement for a strong adhesion. Surface energy depends on the roughness, chemical composition and hydrophilicity/hydrophobicity of the substrate [1,33] and

is easily determined via contact angles measurements and mathematical formulas [32].

Ceramic surface energy is increased after performing hydrofluoric acid etching due to the removal of the low energy contaminants while increasing materials surface roughness [34–36]. In the present study, silanization of previously etched ceramic (RL and CP), reduced the materials' surface energy (Table 3). When etched, ceramic surface is activated increasing the density of hydroxyl groups [9] and surface energy. This high energy on the solid tends to form bonds with other atoms that are close to the surface, to achieve the lowest energy state [37]. After silane application, the energy balance is modified because MPTS molecules will bond to Si−OH on the surface reducing back the ceramic surface energy.

MB groups presented the lowest surface free energy regardless of the silanization protocol. This primer also produced a less pronounced etching pattern compared to that induced by the hydrofluoric acid (RL and CP) (Fig. 2). Low surface roughness produced by MB might have decreased ceramics' wettability, as reported previously [24]. Moreover, surface energy is also related to the chemical composition of the substrate. Fluoride was identified on MB treated specimens even after the washing protocol recommended by the manufacturer [24,25]. The presence of fluoride seems to have some potential to reduce the wettability of the substrate [38], which may explain the decreased on SFE of MB treated groups compared to its control (NS). This lower surface free energy might also be an indicative that silane molecules remains effectively bonded to the available hydroxyls on ceramic surface.

Both CP and RL groups were etched with hydrofluoric acid prior to the application of the primers, but CP groups presented lower surface free energy compared to RL. In addition, the application of CP produced an alteration on ceramics' surface morphology which was not noticed on the group treated with RL (Fig. 2). It seems that a layer was formed when applying CP within the microporosites previously produced by the hydrofluoric acid were reduced. MDP molecules might be filling these surface irregularities while covering some pendent methacrylate groups of the MPTS molecule which may interfere in the proper bonding of the silane layer with the resin cement. This reduction on surface roughness might have helped decreasing the surface free energy on CP treated groups.

Hydrophobicity/hydrophilicity of the silanized ceramic is other important factor that influences the wettability of the resin cement and is an indicator of the efficacy of the silane solution [12]. Glass ceramic surfaces present intrinsic hydrophilic characteristics due to the presence of hydroxyl groups [39] which may induce high wettability of the silane solution. MPTS reacts with hydroxyl groups on silica-rich ceramic surface and with other silanol oligomers forming a branched hydrophobic layer [1]. The formation of this cross-linked structure increases hydrolytic stability of this layer and enhances the penetration of the hydrophobic luting cement into the microporosities of the previously etched ceramic surface, facilitating mechanical interlocking [12,25]. The quality of this layer is not only influenced by the characteristics or composition of the primer, it is also influenced by the method of application [13]. A proper post-silanization protocol might assure the removal of solvents and contaminants in order to increase cross-linking within the silane layer and increase the amount of available reaction sites on the ceramic surface.

Our results demonstrated that in general the different post-silanization protocols produced similar SFE. However, for RL and CP primers the application of a hot stream air (HT) and washing the silanized surface with water at room temperature (WT) resulted in a more hydrophobic layer increasing water contact angles (Fig. 1). This is an indicative that the hydrophilic portion (Si−OH) of MPTS molecules successfully formed Si–O–Si bonds with the lithium disilicate surface and within itself [33], turning ceramics' hydrophilic surface into a more hydrophobic substrate [12]. Otherwise, MR protocol used on RL resulted in lower contact angles similar to not silanized specimens, indicating a limited formation of chemical bonds between the substrate and the silane molecules [33]. This probably occurred due to higher water content as solvent on RL solutions, requiring then longer drying times to be removed, compared to the ethanol present on CP which may be easily volatilized. In the case of MB, no statistical differences were found among the different protocols applied. The manufacturer recommends that when applied, the product must be left in contact with the ceramic surface to let it react and then it must be washed with water [23]. This step is required to remove the acid etchant and reaction byproducts leaving only a thin layer of silane that is chemically bond with ceramic surface. It seems that the water washing step is being effective in removing residuals and so, an additional treatment might not be necessary.

Survey spectra of XPS analysis revealed the presence of F 1s on MB treated specimen (Table 4). This is in accordance with previous studies that identified fluoride even after the ceramic surface has been washed [25,40]. F could be present as part of silica-fluoride salts, probably formed after the reaction of MB with the glassy phase or trapped within the silane layer [25]. Our results demonstrated that F 1s presented a component peak close to 686.4 ± 0.1 eV that can be attributed to fluoro(diethoxy)phosphine [41]. It seems that fluorine remain trapped and bonded within the silane layer and as a result, there is an increase in hydrophobicity and hydrolytic stability of the ceramic-resin cement interface, which might explain the positive performance of MB on the current study [42,43]. However, the significance of this residue is still not clear.

In the high resolution Si 2p XPS spectra (Fig. 3), the binding energy is sensitive to the number of O atoms bonded to Si, allowing the differentiation between Si belonging to the SiO_2 substrate and Si from the silane bonded to the silica surface [44–46]. The $Si(\text{-}O)_3$ component peak corresponds to the silane molecule bonded to the silica surface and is observed at 102.1 ± 0.2 eV. Moreover, Si in the SiO_2 substrate has a $Si(\text{-}O)_4$ binding energy around 103.0 ± 0.2 eV [44]. All silanized groups, except RL-MR, presented spectra with both component peaks $Si(\text{-}O)_3$ and $Si(\text{-}O)_4$, indicating the presence of siloxane bonds between silane and ceramic surface. RL-MR presented a single spectrum, similar to the group NS, correspondent to $Si(\text{-}O)_4$. This finding agrees with the previously mentioned results regarding water contact angles for RL-MR which described a highly hydrophilic surface, probably due to a limited formation of chemical bonds between MPTS and the ceramic surface and a deficient elimination of residuals within the silane layer.

The component peak at an energy binding close to 532.0 eV on O1s high resolution spectra (Fig. 4), corresponds to the O signal from the Si–O–Si silica substrate and appeared in all analyzed groups [44]. On the CP treated ceramic, an additional component peak at 533.0 eV was identified and is attributed to physisorbed water on the substrate surface [44]. This water detected within the silane layer formed by CP might be a consequence of the presence of MDP inside this primer, as it could hinder the elimination of solvents and reaction byproducts such as water [47].

The association of different factors might influence the formation of a good quality silane layer and consequently the wettability of the resin cement when attempting to achieve a strong and long-lasting bonding with the ceramic material. Our findings suggest that all analyzed primers could form siloxane bonds with lithium disilicate ceramic surface. However, the use of additional protocols as HT and WT seems to be necessary when RL and CP primers are used. As a limitation of this in vitro study, it can be pointed, that no mechanical tests were performed and thus, further researches might confirm the extent of these findings on mechanical long-term evaluations.

5. Conclusions

Within the limitations of this in vitro study, the following conclusions must be drawn:

1 The application of silane alone (RL) did not modify ceramic surface morphology and resulted in the highest surface free energy, with an indicative of a hydrophilic surface;
2 Self-etching ceramic primer (MB) presented the lowest surface free energy and produced a highly hydrophobic silane layer;
3 Water rising (WT) and heat treatment (HT) protocols are recommended when using silane (RL) and silane + MDP (CP) primers;
4 Chemical bonds (Si–O) between silane molecules and the ceramic surface were identified for all tested primers.

Acknowledgements

This study was financed in part by the Coordenação de Aperfeiçoamento de Pessoal de Nível Superior-Brasil (CAPES) – Finance Code 001. The authors want to thank Brazilian Nanotechnology National Laboratory (LNNano) and Brazilian Center for Research in Energy and Materials (CNPEM) for the structure and support with the X-ray photoelectron spectroscopy analysis.

REFERENCES

[1] Matinlinna JP, Vallittu PK. Bonding of resin composites to etchable ceramic surfaces — an insight review of the chemical aspects on surface conditioning. J Oral Rehabil 2007;34:622–30, http://dx.doi.org/10.1111/j.1365-2842.2005.01569.x.

[2] Gracis S, Thompson VP, Ferencz JL, NRFA Silva, Bonfante EA. A new classification system for all-ceramic and ceramic-like restorative materials. Int J Prosthodont 2015;28:227–35, http://dx.doi.org/10.11607/ijp.4244.

[3] Tian T, Tsoi JKH, Matinlinna JP, Burrow MF. Aspects of bonding between resin luting cements and glass ceramic materials. Dent Mater 2014;30:e147–62, http://dx.doi.org/10.1016/j.dental.2014.01.017.

[4] Hallmann L, Ulmer P, Kern M. Effect of microstructure on the mechanical properties of lithium disilicate glass-ceramics. J Mech Behav Biomed Mater 2018;82:355–70, http://dx.doi.org/10.1016/j.jmbbm.2018.02.032.

[5] Della Bona A. Characterizing ceramics and the interfacial adhesion to resin: II — the relationship of surface treatment, bond strength, interfacial toughness and fractography. J Appl Oral Sci 2005;13:101–9, http://dx.doi.org/10.1590/S1678-77572005000200002.

[6] Matinlinna JP, Lassila LVJ, Özcan M, Yli-Urpo A, Vallittu PK. An Introduction to silanes and their clinical applications in dentistry. Int J Prosthodont 2004;17:155–64.

[7] Della Bona A, Borba M, Benetti P, Pecho OE, Alessandretti R, Mosele JC, et al. Adhesion to dental ceramics. Curr Oral Health Rep 2014;1:232–8, http://dx.doi.org/10.1007/s40496-014-0030-y.

[8] Shen C, Oh WS, Williams JR. Effect of post-silanization drying on the bond strength of composite to ceramic. J Prosthet Dent 2004;91:453–8, http://dx.doi.org/10.1016/j.prosdent.2004.03.007.

[9] Lung CYK, Matinlinna JP. Aspects of silane coupling agents and surface conditioning in dentistry: an overview. Dent Mater 2012;8:467–77, http://dx.doi.org/10.1016/j.dental.2012.02.009.

[10] Matinlinna JP, Lung CYK, Tsoi JKH. Silane adhesion mechanism in dental applications and surface treatments: a review. Dent Mater 2018;34:13–28, http://dx.doi.org/10.1016/j.dental.2017.09.002.

[11] Antonucci JM, Dickens SH, Fowler BO, Xu HH, McDonough WG. Chemistry of silanes: interfaces in dental polymers and composites. J Res Natl Inst Stand Technol 2005;110:541–58, http://dx.doi.org/10.6028/jres.110.081.

[12] Sattabanasuk V, Charnchairerk P, Punsukumtana L, Burrow MF. Effects of mechanical and chemical surface treatments on the resin-glass ceramic adhesion properties. J Investig Clin Dent 2016;8:1–9, http://dx.doi.org/10.1111/jicd.12220.

[13] Queiroz JRC, Benetti P, Özcan M, Oliveira LFC, Della Bona A, Takahashi FE, et al. Surface characterization of feldspathic ceramic using ATR FT-IR and ellipsometry after various silanization protocols. Dent Mater 2012;28:189–96, http://dx.doi.org/10.1016/j.dental.2011.10.009.

[14] Baratto SSP, Spina DRF, Gonzaga CC, Cunha LF, Furuse AY, Baratto Filho F, et al. Silanated surface treatment: effects on the bond strength to lithium disilicate glass-ceramic. Braz Dent J 2015;26:474–7, http://dx.doi.org/10.1590/0103-6440201300354.

[15] Corazza PH, Cavalcanti SCM, Queiroz JRC, Bottino MA, Valandro LF. Effect of post-silanization heat treatments of silanized feldspathic ceramic on adhesion to resin cement. J Adhes Dent 2013;15:473–9, http://dx.doi.org/10.3290/j.jad.a29592.

[16] Monticelli F, Toledano M, Osorio R, Ferrari M. Effect of temperature on the silane coupling agents when bonding core resin to quartz fiber posts. Dent Mater 2006;22:1024–8, http://dx.doi.org/10.1016/j.dental.2005.11.024.

[17] Carvalho RF, Martins MEMN, Queiroz JRC, Leite FPP, Özcan M. Influence of silane heat treatment on bond strength of resin cement to a feldspathic ceramic. Dent Mater J 2011;30:392–7, http://dx.doi.org/10.4012/dmj.2010-137.

[18] Yavuz T, Eraslan O. The effect of silane applied to glass ceramics on surface structure and bonding strength at different temperatures. J Adv Prosthodont 2016;8:75–84, http://dx.doi.org/10.4047/jap.2016.8.2.75.
[19] Yoshihara K, Nagaoka N, Sonoda A, Maruo Y, Makita Y, Okihara T, et al. Effectiveness and stability of silane coupling agent incorporated in 'universal' adhesives. Dent Mater 2016;32:1218–25, http://dx.doi.org/10.1016/j.dental.2016.07.002.
[20] Pilo R, Dimitriadi M, Palaghia A, Eliades G. Effect of tribochemical treatments and silane reactivity on resin bonding to zirconia. Dent Mater 2018;34:306–16, http://dx.doi.org/10.1016/j.dental.2017.11.006.
[21] Yao C, Yu J, Wang Y, Tang C, Huang C. Acidic pH weakens the bonding effectiveness of silane contained in universal adhesives. Dent Mater 2018;3:809–18, http://dx.doi.org/10.1016/j.dental.2018.02.004.
[22] Ikemura K, Tanaka H, Fujii T, Deguchi M, Negoro N, Endo T, et al. Design of a new, multi- purpose, light-curing adhesive comprising a silane coupling agent, acidic adhesive monomers and dithiooctanoate monomers for bonding to varied metal and dental ceramic materials. Dent Mater J 2011;30:493–500, http://dx.doi.org/10.4012/dmj.2011-012.
[23] Volkel T, Braziulis E, Consulted on Oct 24th, 2018 on Monobond Etch & Prime, scientific documentation; 2015 www.ivoclarvivadent.com.
[24] Tribst JPM, Anami LC, Özcan M, Bottino MA, Melo RM, Saavedra GSFA. Self-etching primers vs acid conditioning: impact on bond strength between ceramics and resin cement. Oper Dent 2018;43:372–9, http://dx.doi.org/10.2341/16-348-L.
[25] El-Damanhoury HM, Gaintantzopoulou MD. Self-etching ceramic primer versus hydrofluoric acid etching: etching efficacy and bonding performance. J Prosthodont Res 2018;62:75–83, http://dx.doi.org/10.1016/j.jpor.2017.06.002.
[26] Lopes GC, Perdigão J, Baptista D, Ballarin A. Does a self-etching ceramic primer improve bonding to lithium disilicate ceramics? Bond strengths and FESEM analyses. Oper Dent 2018;14, http://dx.doi.org/10.2341/17-355-L.
[27] Lyann SK, Takagakib T, Nikaidoc T, Uod M, Ikedae M, Sadrf A, et al. Effect of different surface treatments on the tensile bond strength to lithium disilicate glass ceramics. J Adhes Dent 2018;20:261–8, http://dx.doi.org/10.3290/j.jad.a40632.
[28] Prado M, Prochnow C, Marchionatti AME, Baldissara P, Valandro LF, Wandscher VF. Ceramic surface treatment with a single-component primer: resin adhesion to glass ceramics. J Adhes Dent 2018;20:99–105, http://dx.doi.org/10.3290/j.jad.a40303.
[29] Wu S. Polar and nonpolar intercations in adhesion. J Adhes 1973;5:39–55, http://dx.doi.org/10.1080/00218467308078437.
[30] Dal Piva AMO, Contreras LPC, Ribeiro FC, Anami LC, Camargo SEA, Jorge AOC, et al. Monolithic ceramics: effect of finishing techniques on surface properties, bacterial adhesion and cell viability. Oper Dent 2018;43:315–25, http://dx.doi.org/10.2341/17-011-L.
[31] Combe EC, Owen BA, Hodges JS. A protocol for determining the surface free energy of dental materials. Dent Mater 2004;20:262–8, http://dx.doi.org/10.1016/S0109-5641(03)00102-7.
[32] Inoue N, Tsujimoto A, Takimoto M, Ootsuka E, Endo H, Takamizawa T, et al. Surface free-energy measurements as indicators of the bonding characteristics of single- step self-etching adhesives. Eur J Oral Sci 2010;118:525–30, http://dx.doi.org/10.1111/j.1600-0722.2010.00771.x.
[33] Chen L, Shen H, Suh BI. Effect of incorporating BisGMA resin on the bonding properties of silane and zirconia primers. J Prosthet Dent 2013;110:402–7, http://dx.doi.org/10.1016/j.prosdent.2013.04.005.
[34] Marshall SJ, Bayne SC, Baier R, Tomsia AP, Marshall GW. A review of adhesion science. Dent Mater 2010;26:e11–6, http://dx.doi.org/10.1016/j.dental.2009.11.157.
[35] Yoshida F, Tsujimoto A, Ishii R, Nojiri K, Takamizawa T, Miyazaki M. Influence of surface treatment of contaminated lithium disilicate and leucite glass ceramics on surface free energy and bond strength of universal adhesives. Dent Mater J 2015;34:855–62, http://dx.doi.org/10.4012/dmj.2015-123.
[36] Ramakrishnaiah R, Alkheraif AA, Divakar DD, Matinlinna JP, Vallittu PK. The effect of hydrofluoric acid etching duration on the surface micromorphology, roughness, and wettability of dental ceramics. Int J Mol Sci 2016;17:822, http://dx.doi.org/10.3390/ijms17060822.
[37] Matinlinna JP. Handbook of oral biomaterials. Singapore: Pan Stanford Publishing; 2014.
[38] Baier RE. Principles of adhesion. Oper Dent 1992;(supplement 5):1–9.
[39] Brito e Abreu S, Skinner W. Determination of contact angles, silane coverage, and hydrophobicity heterogeneity of methylated quartz surfaces using ToF-SIMS. Langmuir 2012;28:7360–7, http://dx.doi.org/10.1021/la300352f.
[40] Murillo-Gómez F, Palma-Dibb RG, De Goes MF. Effect of acid etching on tridimensional microstructure of etchable CAD/CAM materials. Dent Mater 2018;34:944–55, http://dx.doi.org/10.1016/j.dental.2018.03.013.
[41] Fluck E, Weber D. P_{2p} binding energies in phosphorus(III) compounds, phosphonium salts and oxyacids of phosphorus. Z Naturforsch 1974;29b:603–7.
[42] Nihei T, Kurata S, Kondo Y, Umemoto K, Yoshino N, Teranaka T. Enhanced hydrolytic stability of dental composites by use of fluoroalkyltrimethoxysilanes. J Dent Res 2002;81:482–6.
[43] Yang F, Zhu L, Han D, Li W, Chen Y, Wang X, et al. Effects of fluorine and silicon components on the hydrophobicity failure behavior of acrylic polyurethane coatings. J Coat Technol Res 2017;14:691–9, http://dx.doi.org/10.1007/s11998-016-9887-0.
[44] Shircliff RA, Stradins P, Moutinho H, Fennell J, Ghirardi ML, Cowley SW, et al. Angle-resolved XPS analysis and characterization of monolayer and multilayer silane films for DNA coupling to silica. Langmuir 2013;29:4057–67, http://dx.doi.org/10.1021/la304719y.
[45] O'Hare LA, Parbhoo B, Ledley SR. Development of a methodology for XPS curve-fitting of the Si2p core level of siloxane materials. Surf Interface Anal 2004;36:1427–34, http://dx.doi.org/10.1002/sia.1917.
[46] Alfonsetti R, Lozzi L, Passacantando M, Picozzi P, Santucci S. XPS studies on SiO_x, thin films. Appl Surf Sci 1993;70/71:222–5, http://dx.doi.org/10.1016/0169-4332(93)90431-A.
[47] Murillo-Gómez F, Goes MF. Effect of different silane-containing solutions on Glass-Ceramic/Cement bonding interacting with dual-cure resin cements. Odovtos Int J Dent Sc 2014;16:87–105, http://dx.doi.org/10.15517/IJDS.V0I16.20330.